Korean J. Crystallography
Vol. 16, No. 2, pp.89~101, 2005

ALD of Nanometal Films and Applications for Nanoscale Devices

Hyungjun Kim
Department of Materials Science and Engineering, Pohang University of Science and Technology (POSTECH), Pohang, Gyungbuk 790-784, Korea

Abstract

Among many material processing related issues for successful scaling down of devices for the next 10 years or so, the advanced gate stack and interconnect technology are two most critical research areas, which need technical innovation. The introduction of new metallic films and appropriate processing technologies are required more than ever. Especially, as the device downscaling continues well into sub 50 nm regime, the paradigm for metal nano film deposition technique research has been shifted to high conformality, low growth temperature, high quality with uniformity at large area wafers. Regarding these, ALD has sparked a lot of interests for a number of reasons. The process is intrinsically atomic in nature, resulting in the controlled deposition of films in sub-monolayer units with excellent conformality. In this paper, the overview on the current issues and the future trends in device processing technologies related to metal nano films as well as the R&D trends in these applications will be discussed. The focus will be on the applications for metal gate, capacitor electrode for DRAM, and diffusion barriers/seed layers for Cu interconnect technology.

1. Introduction

According to ITRS roadmap, the Si semiconductor device processing technology entered 90 nm technology node, which will reach 45 nm in 5~6 years.[1] Figure 1 shows the half pitch trends published in ITRS 2003 roadmap. With the scaling down of the devices, atomic layer deposition (ALD) has been identified as one of the most promising thin film deposition techniques to enable the nanoscale device fabrication, due to its benefits over other conventional deposition techniques including physical vapor deposition (PVD) and chemical vapor deposition (CVD).[2,3] The benefits include the ability to control thickness at atomic scale, ability to produce highly conformal films, and wide area uniformity.[3] Among these, the production of highly conformal film on very small feature size has been considered as one of the biggest benefits, especially for back end of the line (BEOL) process. In contrast to the FEOL applications, where the high k by ALD has been intensively studied, the metal and conducting nitrides are important materials group to

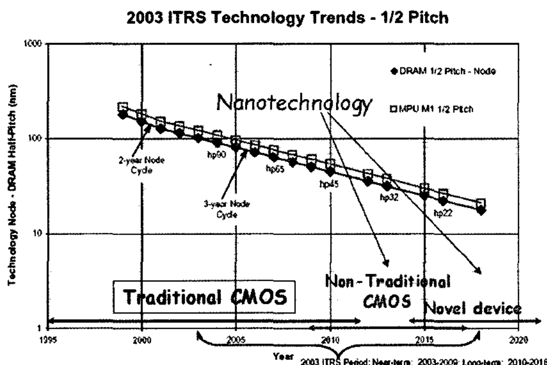

Fig. 1. The half pitch trends in ITRS 2003.

be studied. In fact, the metal nano thin films also have important applications for a front end process as gate electrode for CMOS devices as well as memory applications including capacitor electrode. In this paper, I will discuss the overview on ALD of metal nano films and the applications of these materials in the fabrication of nano scale devices. After brief introduction of the technology, some of the typical experimental results and discussions will

be given focusing on ALD of diffusion barrier and seed layer for Cu.

2. Basics of ALD

Atomic layer deposition of metals and/or nitrides consists of essentially four steps; 1) metal precursor exposure, 2) evacuation or purging of the precursors and any byproducts from the chamber, 3) exposure of the other reactant species (non-metal precursor), for example nitrogen containing reducing agents for nitrides or reducing agents for metals, and 4) evacuation or purging of the reactants and byproduct molecules from the chamber. While the primary reaction between metal precursor and non-metal precursor occurs during step 3), reaction byproducts are also potentially formed at the metal precursor exposure step (step 1). As an example of ALD process, a schematic representation of TiN ALD using $TiCl_4$ as metal precursor and NH_3 as the reducing agent/nitrogen source, which has been one of the most widely studied nitride ALD processes, is shown in Fig. 2. Most other metal or nitride ALD sequences consist of generally similar process steps.

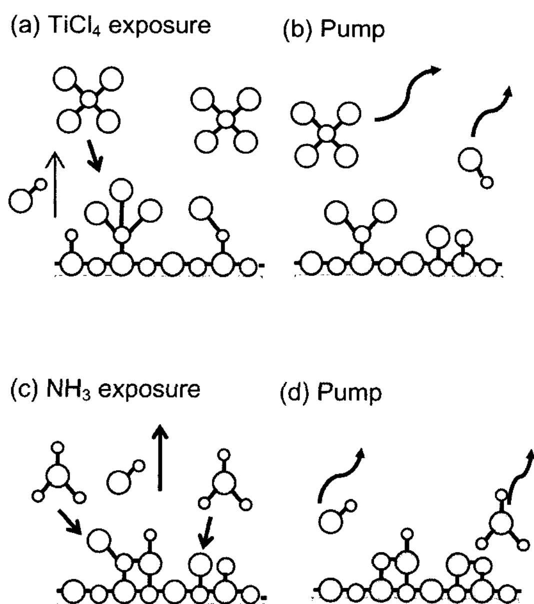

Fig. 2. The schematic representation of each process step for TiN ALD using $TiCl_4$ and NH_3 precursors. (a) $TiCl_4$ exposure, (b) pump out/purge, (c) NH_3 exposure, and (4) pump out/purge step.

As a first step of TiN ALD, the nominally clean initial surface is exposed to $TiCl_4$ for a given time (Fig. 2a). For the case of a liquid source such as TiCl4, the vapor pressure is high enough even at room temperature such that the precursor can be directly admitted to the chamber through a leak valve. In the cases of the most solid precursors, however, it is necessary to heat the chemicals to produce an adequate vapor pressure. One of the most important requirements for this first step is the self-limitation for the precursor molecule adsorption process, usually satisfied by the ligands bonded to the metal atoms in the precursors, such as halogen or organic ligands. This limits further adsorption of the metal precursor by passivating the adsorption sites after the saturation coverage, roughly one monolayer or less, is reached. As Fig. 2a shows, TiCl4 molecules do not adsorb on the surface sites covered by Cl atoms.

At the second step, the remaining precursor gas and any byproducts ($TiCl_4$ and HCl in this example) in the chamber are evacuated. (Fig. 2b) Usually, a purging gas such as argon or nitrogen is used to help complete removal of precursors and/or byproducts. The use of purging gas also helps the elimination of potential CVD-like processes, which can occur when the reactant gas is introduced in the presence of the precursor in the gas phase. This perturbs the ALD growth mode and leads to potential inclusion of byproduct species in the film, as well as the loss of conformality. While the chemistry of the CVD-like process is intrinsically similar to ALD, the fundamental advantages of the ALD approach in terms of thickness and composition control and film uniformity are such that the CVD mode is generally avoided in most cases. At the third step, non-metal precursor (NH3 in this example) is introduced into the chamber. (Fig. 2c) For these non-metal reactant species, which are usually gas phases, MFC or a switched leak valve is used for the control of the flow. In this process, N atoms bond to the Ti on the substrate, resulting in TiN deposition. For metal deposition, a reducing agent such as atomic H is

used for removing Cl from the surface generating fresh surface for further adsorption at the next deposition cycle. At the fourth and last step, all the remaining NH_3 (or hydrogen) and HCl are swept away by evacuation or purging (Fig. 2d).

There are many similarities between ALD and CVD. For example, both techniques use often identical gas phase precursors and chemical reactions between them are the primary thin film deposition mechanism. Accordingly, the physical configuration of the ALD and CVD reaction chambers is usually very similar. In fact, ALD can be thought as a modified version of CVD and for this reason ALD has been also called Atomic Layer CVD (ALCVD). However, the clear, distinctive features of ALD include the self-limited growth mode and the alternate, sequential exposure of the precursor and reactants, resulting in several unique characteristics for ALD which are not found in CVD.

For example, the growth rate as a function of sample temperature or precursor flux shows clear differences between the two deposition techniques. For conventional CVD, the growth rate is a strong function of substrate growth temperature at low temperature, where the growth rate is determined by surface reactions (surface reaction limited regime). At high temperature, however, the growth rate becomes constant with respect to the growth temperature if the mass transport or gas phase diffusion does not limit the process. (flux limited regime). However, for a typical ALD process, the growth rate as a function of growth temperature shows a different trend (Fig. 3). For most cases, the growth rate increases with increasing growth temperature at low growth temperature (typically below 150~300°C for most metals and nitrides ALD). This is mainly because the precursor adsorption or reaction between precursor and surface species is a thermally activated process. Thus, the saturation reaction is kinetically limited with low thermal energy, which would lead to impractically long reaction time.[4] For example, deposition rate rapidly drops below 150°C for W ALD from WF_6, which was attributed to the incomplete reaction.[5] When the metal precursors condense on the substrate, however, the apparent trend may show opposite behavior.

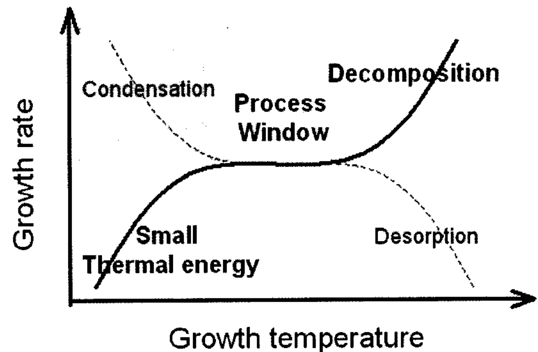

Fig. 3. The typical trends of growth rate as a function of growth temperature for ALD process.

When the ALD process is operated at temperatures providing high enough thermal energy for the chemical reactions, the growth rate usually remains constant with respect to the growth temperature. This temperature range is often called as "ALD process window". However, this terminology could be misleading, since the growth rates weakly depend on the growth temperature even with self-saturation for some cases. Thus, it should be noted that the absence of constant deposition rate as a function of growth temperature does not necessarily mean that the reaction occurs through a non-ALD mode. This almost constant growth rate for some range of growth temperature during ALD provides better reproducibility in film thickness compared to CVD.

At higher growth temperature above this temperature range, however, the growth rate usually increases again with growth temperature, due to the disturbance of self-limitation caused by thermal decomposition of the metal precursor; a "CVD-like" process. While this thermal decomposition problem is not of great concern for halide precursors due to their relatively high thermal stability, metal organic (MO) sources are usually decomposed at relatively low growth temperature. For a few materials systems, the growth rates decrease with increasing growth temperature, when the thermal desorption of deposited materials occurs for example.

The most important benefit of intrinsic self-limitation of ALD is excellent step coverage on aggressive topographic structures, which is the main driving force for the recent intensive interest in ALD for

microelectronics. In an ALD process, the surface saturation effect occurs on all surfaces, which receive an adequate flux of the metal precursor. Thus, with long enough exposure time, nearly 100% conformality in very high aspect ratio (AR=feature depth/width) structures is easily achievable. In contrast, the conformality of PVD technique is intrinsically limited by the directional nature of the sputtered atoms and the near-unity (in many cases) sticking coefficient for the metal atoms.[6] If PVD depositions are made to be very directional as in case of collimated PVD, poor sidewall coverage is resulted on deep features. If the directionality is reduced, sidewall coverage can be increased but there is a tendency to produce overhangs in the deposited films near the top corners of features, which can limit subsequent process steps. Because of the directional nature of PVD, conformality is limited to usually less than 20%.

Although CVD can produce better conformality than PVD in some systems, there is an intrinsic flaw relating conformality to film composition or continuity in very thin films. Due to the flux-controlled nature of CVD, conformality in deep features can only be achieved with a low reaction probability (at low growth temperature of surface reaction limited regime). This same feature inhibits film nucleation and can result in poor continuity at the sub-5nm thickness regime desired for many applications. In addition, the low reaction rate can lead to impurity incorporation either from non-reacted precursors or poor removal of byproducts.

Since ALD is inherently self-limited deposition process by the alternate exposure of two or more precursors, thickness and composition control is feasible at the sub-monolayer or even atomic level. Thus, ALD is an ideal deposition technique to construct nanolaminate structures. ALD has been employed for superlattice structure formation of compound semiconductors from the early history of ALD.

Another characteristic of ALD is the generally lower growth temperature compared to the parallel CVD reaction. Since the adsorbed monolayer is reacted to completion, there is often a much lower impurity level in the deposited film compared with CVD. This is related to the fact that the ALD process occurs exclusively through surface reactions. For CVD, except for several special cases (such as UHV-CVD, for example), vapor phase chemical reaction is the main reaction mechanism, which is a common source of particle formation in CVD reactors. In addition, since ALD occurs through surface reaction, the selectivity of deposited materials could be controlled by proper selection of precursors and surface preparation.

The growth rate of ALD is very low compared to virtually all other deposition techniques. In general, the thickness/cycle in the typical ALD mode is limited to below 1 ML/cycle. For practical vacuum systems, the total time for 1 cycle (4 steps) is mostly longer than 1 sec. This corresponds to the deposition rate of 1 μm/hr or below (a few nm/minute). Moreover, the actual deposition thickness/cycle is often a small fraction of a ML per cycle for most metal and nitride ALD. In recent applications in microelectronics, however, the required thickness of metals and nitrides films has become very small, in the low nm range, and this resulted in the low growth rates of ALD more acceptable. For example,

Table 1. The comparison among PVD, CVD, and ALD

	PVD	CVD	ALD
Reaction	Physical adsorption	Surface +vapor reaction	Surface reaction
Growth temperature	Low (RT)	High (>600°C) to middle	Low to middle (<500°C)
Step coverage	Poor	Good	Excellent
Impurity	Very low (<1%)	A few %	Low (<1%)
Thickness control	>50 Å	>10 Å	<a few Å
Particle	OK	poor	OK
Wafer uniformity	Good	Good	Excellent
Growth rate	Fast	Middle	Slow

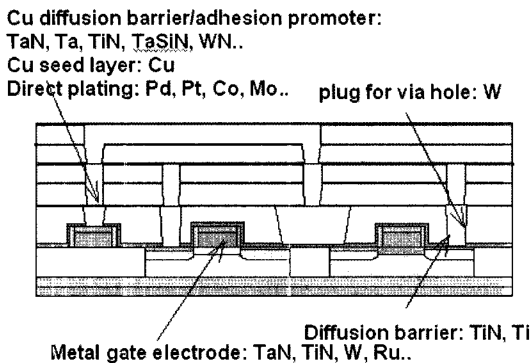

Fig. 4. The applications of metal nanofilms in nanoscale devices.

for the 65 nm interconnect generation, the Cu diffusion barrier thickness can be no more than 5 nm thick, which can be deposited with less than 100 ALD cycles for most cases. Thus, the required film can be grown within a several minutes, leading to a wafer chamber throughput of perhaps 20 wafers per hour (w.p.h.) or more. In summary, Table 1 compares the characteristics of PVD, CVD, and ALD.

Due to these many benefits, ALD of metal and metallic nitride films have been studied for many important applications in nanoscale device fabrications. Figure 4 shows the applications of ALD metal films in modern CMOS fabrications. Various metal films have been deposited by ALD from various precursors and Table 2 summarizes some of the reported results.

3. Cu Interconnect Technology and ALD

Among many potentially important applications of ALD metallic thin films, the applications in Cu interconnect technology is one of the most widely studied applications. As device scales down, RC delay of the devices becomes more and more serious problem. In addition to the intrinsic delay of devices themselves, the portion of interconnect delay is considered to be more problematic. To reduce the RC delay, low resistivity metal lines and low dielectric constant dielectric materials should be employed. Cu has low resistivity, which is second to none to Ag, and the electromigration resistance has been expected to surpass that of Al. Although the implementation of Cu interconnect has been intensively studied from late '80s, the Cu interconnect technology has been succeeded into mass production only from late '90s. There have been several technological enablers for Cu interconnects. The traditional Al(Cu) interconnect has been done by Al layer deposition on plane surface and subsequent RIE of Al to make a pattern. For Cu interconnect, however, reactive ion etching (RIE) has been very difficult due to the lack of volatile halide for Cu. Due to the

Table 2. Reported metals and metallic nitrides ALD

		Precursors	Deposited materials
Inorganic (Halides)		$TaCl_5$, $TaBr_5$ $TiCl_4$, TiI_4 WF_6 $MoCl_5$ $NbCl_5$ CuCl	Ta, TaN, Ta_3N_5, $TaSi_xN_y$ Ti, TiN, $TiSi_xN_y$, $TiAl_xN_y$ W, W_2N, WC_xN_y Mo, MoN_x NbN Cu
Metal organic	Diketonato complexes	$Ni(acac)_2$ $Pt(acac)_2$ $Cu(hfac)_2$, $Cu(thd)_2$	Ni Pt Cu
	Cyclopentadienyl compounds	$Ru(Cp)_2$, $Ru(Od)_3$ $Me(Cp)PtMe_3$ $Ni(Cp)_2$	Ru Pt Ni
	Alkyl compound	TMA	Al
	Alkylamides	TDMAT, TEMAT TBTDET, PEMAT	TiN, $TiSi_xN_y$, $TiAl_xN_y$ TaN

difficulty of Cu etching, new integration scheme, damascene technology, has been introduced. For Cu damascene process, the deposition of Cu into pre-patterned dielectric layer and global planarization of Cu deposition are required. The deposition of Cu into via/trench (which is often called gap filling) has been realized by deposition of Cu using electroplating, and chemical mechanical planarization (CMP) has been successfully employed as effective global planarization process.

Besides the introduction of novel integration process, the Cu has additional difficulties to be used as a wiring metal; Cu is a very fast diffuser and easily go into Si devices or dielectrics and the adhesion of Cu on most of dielectrics is poor. To prevent the diffusion of Cu, effective diffusion barrier layer is required, which should have a good adhesion property also. Due to the same reason, Cu interconnect requires sidewall protection against Cu diffusion. D. Edelstein et al investigated various liners, in terms of important barrier/adhesion layer properties including diffusion barrier property, adhesion, and corrosion resistance etc.[7] The report has shown that TaN/Ta is the most suitable liner, and currently this bilayer structure is the most widely used. This is mainly because while the adhesion between Ta and Cu is good, the adhesion of TaN is superior to that of Ta/dielectric interface. In addition to this liner, the electroplating of Cu requires seed layer since Cu cannot be electroplated directly on diffusion barrier materials due to high resistivity. For this purpose, thin Cu layer is deposited after liner deposition before Cu electroplating.

So far, Cu diffusion barrier and seed layer has been deposited by PVD for this purpose. To enhance the conformality and ensure large enough sidewall coverage, intensive technological improvement has been done for PVD. Currently, ionized PVD (I-PVD) is standard process for liner/seed layer deposition. For the current 90 nm technology node, PVD based deposition is being used and this might be extended to 65 nm. However, in the near future, especially for 45 nm and beyond, very conformal, ultra thin film deposition technique will be required, which may be achievable only by ALD technique. Currently, the thickness of total liner prepared by PVD is in the region of 20 nm or so, which should be decreased to few nm thickness in several years.[1] The main reason is that as the metal pitch decreases further, the volume fraction of higher resistance liner becomes high. Also, as the line width reaches 50 nm or so, the inherent resistivity of Cu becomes higher due to the size effects caused by electron surface scattering.

Currently, Cu seed layer over 300 Å thick (field thickness) is deposited by I-PVD, to ensure thick enough side/bottom coverage. But with 65 nm technology and beyond, much thinner conformal seed layer is required. Cu CVD or ALD has not been successfully developed yet, mainly due to the lack of good metal precursor. Alternatively, Cu electro deposition can be done on other low-resistance conductor layer. The required material properties for this purpose include nobility, formation of soluble or conducting oxides, and insolubility in Cu batch. Preferably, direct plating materials have good diffusion barrier properties as well as good adhesion to dielectrics. A few metal layers have been identified as candidates, which are mostly refractory metals such as Ru, Rh, Co, Mo, Cr, and W. By the implementation of ALD of seed layer, all ALD based liner/seed, which leads to very thin structure but with high performance, will be viable.

4. Experimental Procedures

The detailed description of the ALD system is given in previous reports.[8,9] Ta-based materials have been produced by plasma enhanced ALD (PE-ALD) from chloride and metal organic precursor. The metal organic precursor employed in this study was $Ta[N(Me)_2]_5$ [pentakis(dimethyamino)tantalum, PDMAT]. The solid $TaCl_5$ and PDMAT (powder) source contained in a separate glass tube was used as a metal precursor. The glass tube was maintained at 100°C for $TaCl_5$ and 65°C for PDMAT to develop adequate vapor pressure, and all the delivery lines were heated to a little higher temperature than source. Ar was used as carrier gas and the flow was controlled by a leak valve upstream from the source tube. Atomic hydrogen and/or activated N_2 are generated by a quartz tube connected to the sample

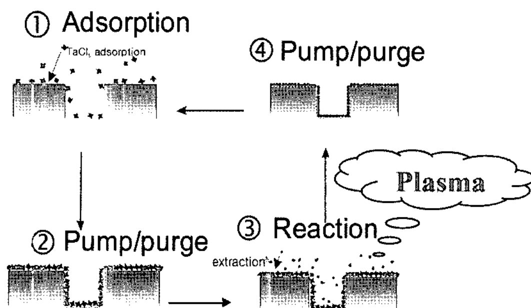

Fig. 5. Schematic drawing of typical PE-ALD process. Here, Ta PE-ALD from $TaCl_5$ has been shown as an example.

chamber via a gate valve and hydrogen and nitrogen gases are supplied via a leak valve. The deposition cycle consists of the following steps: exposing the substrate to metal precursor vapor carried by Ar gas for a given time, evacuating the chamber, opening the hydrogen and nitrogen source valves and initiating the RF plasma for a set time, and shutting off the hydrogen and nitrogen sources and the plasma, allowing the chamber to return to base pressure. The schematic drawing for Ta PE-ALD process is shown in Fig. 5 as an example. The overall process is almost same as that of thermal ALD, except that plasma is turned on during the exposure step of reactant gas, in this example hydrogen. For TaN deposition, nitrogen is simultaneously introduced to produce the mixture of atomic hydrogen and activated nitrogen. For Ru ALD, the same process chamber has been used although plasma activation was not employed. The Ru precursor was metal organic precursor which has similar structure with bis(cyclopentadienyl)Ru ($Ru(Cp)_2$). The Ru ALD already has been demonstrated previously, using bis(cyclopentadienyl)Ru and $Ru(Od)_3$ [Od= 2,4-octanedionate] and molecular oxygen as oxidative.[10,11] The approximate exposure time for each step was 2 sec Ru precursor, 1 sec of pumping out, 2 sec of oxygen exposure and 1 sec of pumping out.

The PE-ALD Ta or TaN films were deposited on HF-dipped Si(001) or 5000 Å thermally SiO_2 grown on Si substrates. The film composition and thickness were determined by Rutherford backscattering spectrometry (RBS). In addition to measuring the N/Ta ratio for TaN, RBS was also used to determine impurity content, such as Cl, C and O. The microstructures of the thin films were investigated using X-ray diffraction and transmission electron microscopy (TEM). Surface roughness was measured by atomic force microscope (AFM).

For Cu diffusion barrier measurements, a 200 nm PVD Cu layer was deposited on top diffusion barrier, without breaking vacuum, using a power level of 1 kW (dc) in the UHV sputtering system. The pressure during the Cu deposition was 5 mTorr. The Ta or TaN films described above were deposited on HF-dipped polycrystalline Si substrates. A SiO_2 buffer layer placed between the poly-Si and Si (100) was used to electrically isolate the Si(100) substrate during the sheet resistance analysis. Copper diffusion barrier failure was studied using three different *in situ* techniques, including synchrotron XRD, optical scattering, and sheet resistance measurements, conducted simultaneously, while the samples were annealed at a temperature ramp rate of 3°C/s from 100 to 1000°C in He environment. The detailed description of the analysis technique can be found at the previous reports.[12]

5. Results and Discussions

5-1. PE-ALD of diffusion barriers for Cu interconnect technology

The PE-ALD of Ta and TaN from $TaCl_5$ has been previously reported by the current author.[8,9] Here, I summarize the important aspects of the results. To indicate the typical deposition characteristic, the deposition rate vs $TaCl_5$ exposure time has been shown in Fig. 6. Here, the deposition rate was represented by the number of Ta atoms/cycle, determined by RBS. Initially the deposition rate increases abruptly with increasing $TaCl_5$ exposure time up to about 1 sec of exposure time. But with further increase in exposure time did not increase the deposition rate, saturating at 0.08 Å/cycle. Similar results were obtained for TaN PE-ALD from $TaCl_5$ and PDMAT, although the deposition rate at saturation conditions were higher as 0.24 Å/cycle and 0.31 Å/cycle, respectively. This saturation behavior is a unique characteristic of ALD, indicating the self-

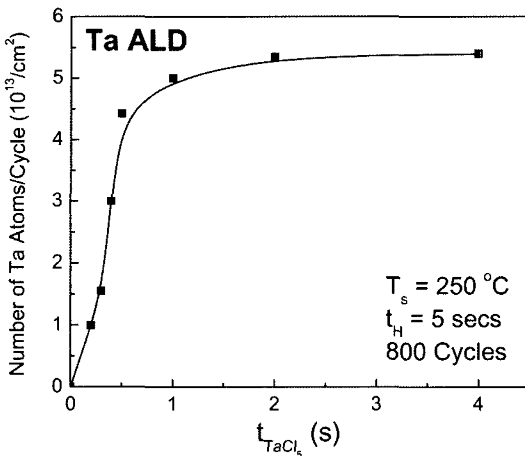

Fig. 6. The deposition rate of Ta PE-ALD from $TaCl_5$ and atomic H as a function of $TaCl_5$ exposure time to illustrate the self-saturated adsorption of metal precursor. The growth temperature was 250°C.

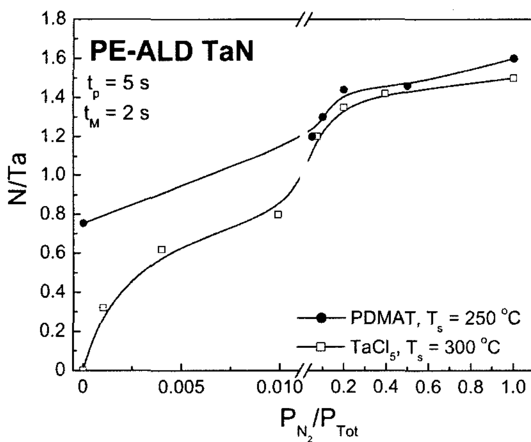

Fig. 7. N/Ta ratio in PE-ALD TaN measured by RBS as a function of nitrogen partial pressure during plasma exposure. PDMAT process is denoted as filled circle and $TaCl_5$ process is denoted as open square.

saturated adsorption of metal precursor. Once the saturation coverage is reached, no further adsorption occurs.

One of the important results for TaN PE-ALD from PDMAT and $TaCl_5$ is the nitrogen content in the film with increasing nitrogen flow during deposition. The N/Ta ratios in the films, measured by RBS, are shown in Fig 7. For $TaCl_5$ precursor, the nitrogen content in the film is 0 with hydrogen only plasma, with increasing nitrogen flow, the nitrogen content in the film increases continuously. With nitrogen only plasma, the deposited film has N/Ta ratio of 1.5, close to that of Ta_3N_5 phase. More detailed results are found on the previous report.[6] But for PDMAT, the nitrogen content in the film is higher than 0.7, even without addition of nitrogen in the plasma. This is attributed to the nitrogen incorporation from metal precursor itself. The nitrogen in PDMAT, originally bonded to Ta, is incorporated without extra nitrogen provision. Similar results were obtained for PE-ALD of TaN from tert-butylimidotris(diethylamido)tantalum (TBTDET) and atomic hydrogen.[13] But with nitrogen plasma only, the N/Ta ratio in the film is similar to that from $TaCl_5$.

The deposition temperatures were about 300°C for $TaCl_5$ and 250°C for PDMAT, which were determined by separate deposition experiments at various temperatures. In this standard condition, the Cl content in the TaN from $TaCl_5$ was below 0.5 at%, while the carbon content in the TaN from PDMAT is about above 10 at%. This high carbon content is attributed to the carbon incorporation from thermal/plasma dissociation of methyl ligand in PDMAT. In this study, we did not try to decrease the carbon content, so it may be reduced further by optimization. At stoichiometric composition, the resistivity was 200~300 μΩcm for $TaCl_5$, and 300~500 μΩcm for PDMAT, which further increase to very high value with increasing nitrogen content. The resistivity of thermal ALD TaN layer from MO precursor and NH_3 was reported to be very high.[13] The low resistivity of PE-ALD TaN from hydrogen plasma is mainly due to the low nitrogen content in the film, and possibly due to the formation of low resistivity TaC phase, as reported previously.[13] For both cases, the conformality was almost 100% for trench structure with aspect ratio of 10 : 1.

The microstructures of three cases, PE-ALD Ta and TaN from chloride and TaN from PDMAT (TaN films with N/Ta=1), were studied by XRD and TEM. PE-ALD Ta films shows amorphous microstructure, while TaN from $TaCl_5$ has well developed polycrystalline structure. However, The XRD and TEM results indicate that the PE-ALD

TaN from PDMAT is mostly composed of cubic TaN nanocrystalline, surrounded by amorphous matrix of Ta rich. The size of nanocrystalline is about 2~3 nm. For all three cases, the AFM measurement of surface roughness shows that the surface is very smooth, with RMS roughness about 0.1 nm.

For Ta and TaN, the failure mechanism as Cu diffusion barrier is known to be similar, mainly determined by Cu diffusion through the layer. The failure of the PVD Ta barrier between Cu and Si is first indicated by η" Cu_3Si formation at the Ta-Si interface caused by the diffusion of Cu through Ta films, followed by accelerated Ta_5Si_3 and $TaSi_2$ formation.[14-16] Similar to Ta layer, the Cu silicide has been observed to form by Cu diffusion through TaN layer.[17-19] Most of the reports on diffusion barrier properties of CVD or ALD TaN layers have been on nitrogen rich phases (such as Ta_3N_5) or TaN with high impurity levels. For 10 nm cubic Ta(Al)N(C) films, deposited by ALD from $TaCl_5$, NH_3, and TMA, the failure temperature determined by XRD was found to be around 600°C for 15 minutes of annealing time.[20] For nitrogen rich TaN_x layers deposited by thermal CVD either from halide ($TaBr_5$) or MO (TBTDET) precursors, lower Cu diffusion barrier failure temperatures were obtained compared to PVD TaN_x.[21-23] The poorer performance of CVD TaNx was explained by the amorphous to crystalline phase (Ta_3N_5) transition,[21] or by the denser structure of PVD TaN films with different preferred orientation.[23]

Most recently, the diffusion barrier property of stoichiometric PE-ALD TaN has been reported by current author.[24] Here, the comparison among PE-ALD Ta and TaN from $TaCl_5$ and MO PE-ALD TaN layers (TaN films with N/Ta=1) will be presented. As mentioned in section III, the barrier failure temperatures for PE-ALD Ta and TaN from $TaCl_5$ and MO PEALD TaN layers were determined by synchrotron XRD, optical scattering, and resistivity measurement for layers with various thickness raging from 2 nm to 15 nm. The barrier failure temperature was determined using the disappearance of the Cu 111 XRD peak; by taking the derivatives of the integrated XRD peak intensity versus annealing temperature, the minima obtained were recorded as

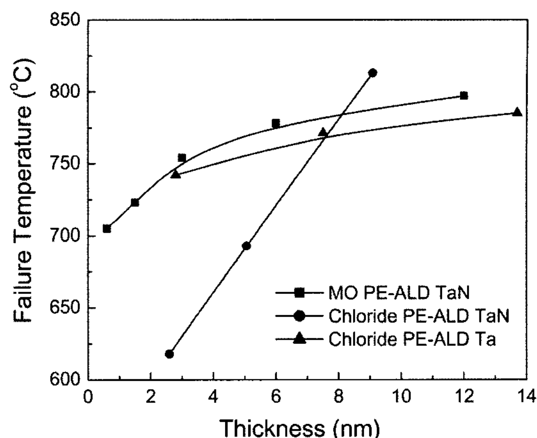

Fig. 8. Cu diffusion failure temperature as a function of barrier thickness for $TaCl_5$ PE-ALD Ta (triangle), TaN (circle), and Mo PE-ALD TaN (square). The diffusion barrier failure temperatures were measured by synchrotron XRD as described in the text.

the barrier failure temperature. More detailed results for PE-ALD Ta is found in the previous report.[8] Without any diffusion barrier, the reaction between Cu and Si occurs around 260°C, indicated by the rapid increase of resistivity, optical scattering as well as the disappearance of Cu XRD peak accompanied by appearance of Cu silicide peak. (Data not shown) However, with the presence PE-ALD Ta or TaN, the failure temperature is raised to 600~800°C range, indicating that these layers are good diffusion barriers. The failure temperatures as a function of barrier thickness for three different PEALD films are shown in Fig. 7. For PE-ALD TaN from $TaCl_5$, the failure temperature decreases more rapidly with reduced thickness compared to the other two cases. Thus, at very thin films under 8 nm, the failure temperature of PE-ALD TaN from $TaCl_5$ is lowest.

Activation energy for Cu diffusion for these barriers were obtained by using simple kinetic equations, as described in ref. 9. The activation energy for polycrystalline TaN from $TaCl_5$ obtained from the present study, 1.2 eV, is very close to that for grain boundary diffusion (1.3 eV).[18] Thus, we concluded that the Cu diffusion barrier failure for the PE-ALD TaN layers from $TaCl_5$ in the present study is dominated by grain boundary diffusion, which is expected based upon their polycrystalline micro-

structure. Meanwhile, E_a for PE-ALD Ta from $TaCl_5$ and PE-ALD TaN from PDMAT, which have amorphous or nanocrystalline in amorphous matrix structure, were estimated as 5.4 and 5.3 eV, respectively. These high activation energy values indicate that the Cu diffusion through these barriers is dominated by bulk diffusion. Thus, we can conclude that the microstructure of the barrier materials is one of the most critical factors determining Cu diffusion barrier performance and as the diffusion barrier becomes thinner with the downscaling of the devices, the control of film microstructure becomes more important. And the bilayer structure composed of PE-ALD nanocrystalline TaN barrier by MO precursor and PE-ALD Ta from $TaCl_5$ is very promising diffusion barrier for ULSI Cu interconnect technology of 65 nm and beyond. With this combination, ultra thin, nano scale Cu interconnect would be possible.

Additionally, we performed PE-ALD of TaN on top of porous low k materials using PDMAT. One of the biggest challenges for integration of ALD barrier with porous low k materials is the penetration of liner into the nano pores. For example, W ALD on top of porous dielectrics resulted in deep penetration of W, which causes leakage and unacceptable performance of the devices.[28] There have been several different ways for pore sealing including chemical treatment, plasma surface treatment, and deposition of dielectric liners.[29] Still, there has been no clear solution for this problem. From TEM study (data not shown) for PE-ALD TaN without any surface treatment we did not observe any evidence of TaN penetration into various porous low k dielectris. The exact reason of penetration prevention during PE-ALD is not clearly known. However, we can qualitatively explain the results based upon the difference of reaction mechanism between thermal and PE-ALD. For PE-ALD, the reactant to remove ligands producing metal layer is atomic hydrogen and activated nitrogen. It is known that the hydrogen atoms rapidly recombine with the existence of surfaces. In the inside of nano pores of porous low k materials, the radicals will quickly recombine, and only a small fraction of radicals would reach deep into the pores. So although the metal precursor will go into the inside of pores, the reaction does not essentially occur. Meanwhile, on the outside surface, deposition continuously proceeds, leading to closing of pores and self-pore sealing by PE-ALD. Additionally, there may be pore sealing effect by plasma used for ALD. Thus, PE-ALD seems to have additional benefit over thermal ALD in terms of integration with porous low k by effectively reducing the linier penetration.

5-2. Ru ALD for seed layer

Recently, Ru is receiving intensive attention due to its good properties as electrode in DRAM applications, and metal gate for CMOS in addition to the application as a seed layer for direct plating of Cu.[29] A simple way of depositing metallic Ru by ALD has been reported recently.[10,11] $Ru(Cp)_2$ and $Ru(Od)_3$ were used as a metal precursor which reacted with O_2 to produce Ru thin films in an ALD mode. The Ru ALD process was explained by the oxidative decomposition of Ru precursor ligands, producing CO_2 and H_2O as byproducts. Polycrystalline Ru films with low resistivity (17~18 μΩcm) were deposited on *in-situ* grown ALD Al_2O_3 and TiO_2 layer.[10] On a SiO_2 surface, however, the deposited films were nonuniform with macroscopic defects. This was attributed to the difference in the surface density of hydroxyl group, which promote uniform nucleation of Ru films on an oxide surface. The reported impurity levels in the films were quite low (H, C, O<1 at%) and RuO_2 was not deposited with the studied experimental conditions.

Ru ALD has been performed on PE-ALD TaN layer. More detailed study has been reported in ref. 30. Here, only some of the essential results are described. XRD spectra of ALD Ru thin films indicated that only metallic Ru film is deposited without any formation of Ru oxide. The nucleation of Ru on top of PE-ALD TaN layer was good, and the thickness versus number of cycles did not show any indication of nucleation period. Previously, it was reported that the Ru ALD requires Al_2O_3 or TiO_2 to obtain films with good uniformity and without macroscopic hole.[10] Our results indicate that the freshly grown PE-ALD TaN provides good nucleation sites for Ru ALD, leading to quite uniform layer over

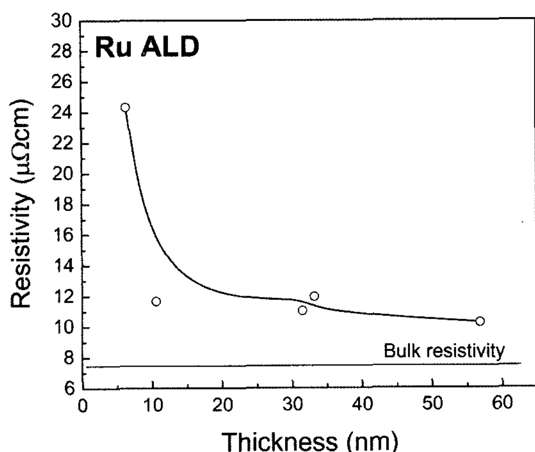

Fig. 9. The resistivity of ALD Ru as a function of film thickness. The deposition temperature was 300°C.

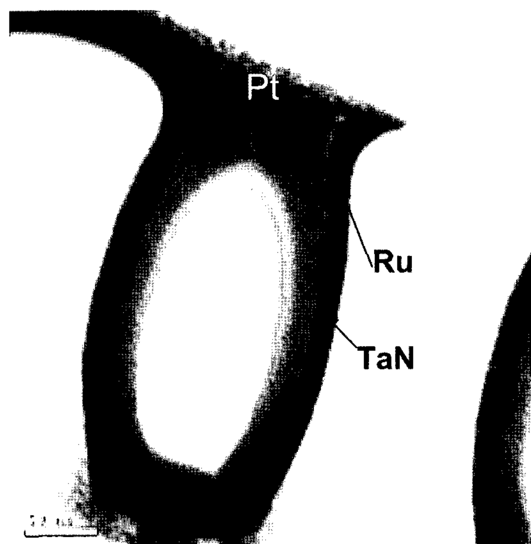

Fig. 10. 15 Å PE-ALD TaN/200 Å ALD Ru deposited in trench structure of porous low k, showing the possibility of all ALD based liner/seed structure.

200 mm wafers. The carbon content was below the detection limit of RBS, and oxygen content was very low, below 0.5%, at typical deposition condition of 300°C. The deposition rate was about 1~1.1 Å/cycle, which is higher than the previous report, probably due to the difference in Ru precursor. The surface roughness was about 6 Å for 200 Å films, which are higher than those for PE-ALD Ta and TaN. Fig. 9 is the resistivity of ALD Ru films as a function of film thickness. Up to thickness of 10 nm, the resistivity remains low at about 10~12 μΩcm. Although this value is higher than that of bulk Ru, the resistivity is lower than typical value of Ru deposited by CVD and previous reported value deposited by ALD. Diffusion barrier test has been performed for bilayer of 5 Å TaN and 100 Å Ru layer, by the same analysis technique mentioned above. The barrier failure occurs at about 700°C, which is similar to 5 Å thick TaN layer alone. Thus, we conclude that the Ru layer itself is not an effective diffusion barrier. However, for 5 Å PE-ALD TaN layer alone, weak Cu silicide XRD peak was observed at as low temperature as 450°C, indicating local reaction between Cu and Si. For bilayer of TaN/Ru, this local reaction was prevented, indicating the Ru layer at least improves the diffusion barrier property for ultra thin TaN diffusion barrier.

Figure 10 is a cross sectional TEM image of PE-ALD TaN/ALD Ru bilayer deposited on top of porous SOD trench structure. 15 Å TaN was deposited first and 200 Å Ru was deposited on top of TaN. As shown in the figure, Ru layer was deposited almost conformally in the structure, and TaN layer was deposited without penetration to the porous dielectric layer. This result shows that the integration of TaN diffusion barrier and Ru seed layer, all deposited by ALD, can be integrated successfully with porous low k materials. The initial Cu plating results on top of this bilayer came out good. Thus, ultra thin liner/seed layer by ALD is a viable option for future Cu interconnect, which can lead to the successful integration into 65 nm technology node and beyond.

6. Conclusion

The need for ultra thin, highly conformal metal nanofilms has driven the implementation of ALD technology for nanoscale device fabrications. With further scaling of devices into 65 nm and beyond, the conventional PVD based liner/seed will be slowly, but necessarily, replaced by ALD based layers due to its excellent property including excellent conformality. In this paper, some of the essential features of ALD/PE-ALD of typical metal nano

films were summarized. PE-ALD Ta and TaN layer has been developed for Cu diffusion barrier using $TaCl_5$ and PDMAT as Ta precursors. Due to the microstructure difference, PEALD Ta from $TaCl_5$ and PE-ALD TaN from PDMAT have produced best combination in terms of diffusion barrier failure temperature. PE-ALD liner also has benefits of little penetration into porous low k, which makes possible integration of liner without additional pore sealing process. Ru ALD has been applied to the deposition of Cu plating seed layer. TaN/Ru liner/seed layer was all prepared by ALD with good conformality and indicates the possibility of successful integration into 65 nm technology and above.

Acknowledgments

Lots of these works have been done at IBM T.J. Research center and H. Kim appreciates the help from other colleagues including C. Cabral, Andy Kellock, and C. Lavoie.

References

1) International technology roadmap for semiconductor 2003 ed. http://public.itrs.net.
2) Rossnagel, S. M. and Kim, H., Proceedings of the IEEE 2001 International Interconnect Technology Conference, p3 (2001).
3) Kim, H., *J. Vac. Sci. Technol.*, **B21**, 2231 (2003).
4) Ritala, M. and Leskelä, M., in H. S. Nalwa (Ed.), *Handbook of Thin Film Materials*, vol. 1, Academic Press, San Diego, CA, 2001, p. 103.
5) Klaus, J. W., Ferro, S. J. and George, S. M., *Thin Solid Films*, **360**, 145 (2000).
6) Rossnagel, S. M., *J. Vac. Sci. Technol.*, **B16**, 2585 (1998).
7) Edelstein, D., Uzoh, C., Cabral, C. Jr., DeHaven, P., Buchwalter, P., Simon, A., Cooney, E., Malholtra, S., Klaus, D., Rathore, H., Ararwala, B. and Nguyen, D., Proc. of the IEEE 2001 International Interconnect Technology Conference, p9 (2001).
8) Kim, H., Cabral, C. Jr., Lavoie, C. and Rossnagel, S. M., *J. Vac. Sci. Technol.*, **B20**, 1321 (2002).
9) Kim, H., Kellock, A. J. and Rossnagel, S. M., *J. Appl. Phys.*, **92**, 7080 (2002).
10) Aaltonen, T., Alén, P., Ritala, M. and Leskelä, M., *Chemical Vapor Deposition*, **9**, 1 (2003).
11) Min, Y.-S., Bae, E. J., Jeong, K. S., Cho, Y. J., Lee, J.-H. and Choi, W. B., *Adv. Mater.*, **15**, 1019 (2003).
12) Cabral, C. Jr., Lavoie, C., Harper, J. M. E. and Jordan-Sweet, J., *Thin Solid Films*, **397**, 194 (2001).
13) Park, J.-S., Park, H.-S. and Kang, S.-W., *J. Electrochem. Soc.*, **149**, C28 (2002).
14) Holloway, K., Fryer, P. M., Cabral, C. Jr., Harper, J. M. E., Bailey, P. J. and Kelleher, K. H., *J. Appl. Phys.*, **71**, 5433 (1992).
15) Laurila, T., Zeng, K., Kivilahti, J. K., Molarius, J. and Suni, I., *Thin Solid Films*, **373**, 64 (2000).
16) Clevenger, L. A., Bojarczuk, N. A., Holloway, K., Harper, J. M. E., Cabral, C. Jr., Shad, R. G., Cardone, F. and Solt, L., *J. Appl. Phys.*, **73**, 300 (1993).
17) Min, K.-H., Chun, K.-C. and Kim, K.-B., *J. Vac. Sci. Technol.*, **B14**, 3263 (1996).
18) Oku, T., Kawakami, E., Uekubo, M., Takahiro, K., Yamaguchi, S. and Murakami, M., *Appl. Surf. Sci.*, **99**, 265 (2996).
19) Takeyama, M., Noya, A., Sase, T. and Ohta, A., *J. Vac. Sci. Technol.*, **B14**, 674 (1996).
20) Ritala, M., Kalsi, P., Riihelä, D., Kukli, K., Leskelä, M. and Jokinen, J., *Chem. Mater.*, **11**, 1712 (1999).
21) Kaloyeros, A., Chen, X., Stark, T., Kumar, K., Seo, S.-C., Peterson, G. G., Frisch, H. L., Arkles, B. and Sullivan, J., *J. Electrochem. Soc.*, **146**, 170 (1999).
22) Cho, S.-L., Kim, K.-B., Min, S.-H., Shin, H.-K. and Kim, S.-D., *J. Electrochem Soc.*, **146**, 3724 (1999).
23) Tsai, M. H., Sun, S. C., Tsai, C. E., Chuang, S. H. and Chiu, H. T., *J. Appl. Phys.*, **79**, 6932 (1996).
24) Kim, H., Lavoie, C., Copel, M., Narayanan, V., Park, D.-G. and Rossnagel, S. M., *J. Appl. Phys.*, **95**, 5848 (2004).
25) Rodbell, K. P., Tu, K. N., Lanford, W. A. and Guo, X. S., *Phys. Rev.*, **B43**, 1422 (1991).
26) Shewmon, P., "Diffusion in Solids", 2nd ed. The Minerals, Metals, and Materials Society (1989).
27) Wang, H., Tiwari, A., Zhang, X., Kvit, A. and Narayan, J., *Appl. Phys. Lett.*, **81**, 1453 (2002).

28) Ryan, E. T., Freeman, M., Svedberg, L., Lee, J. J., Guenther, T., Connor, J., Yu, K., Sun, J. and Gidley, D. W., *Proc. MRS 2003 Spring*, **E10**, 8 (2003).
29) Chyan, O., Tiruchirapalli, Z., Arunagiri, N. and Ponnuswamy, T., *J. Electrochem. Soc.*, **150**, C347 (2003).
30) Kim, H., van der Straten, O. and Rossnagel, S. M. in preparation.
31) Kang, S. T., Choi, K. H., Hwang, C. S. and Kim, H. J., *J. Electrochemical Soc.*, **147**, 1161 (2000).